Selecting Suitable Functionals and Basis Sets on the Study Structural and Adsorption of Urea-Kaolinite System Using Cluster Method

Nur Najwa-Alyani Mohd Nabil and Lee Sin Ang*

Faculty of Applied Sciences, Universiti Teknologi MARA, 02600 Arau, Perlis, Malaysia

* ***Corresponding author:***

email: anglee631@perlis.uitm.edu.my

Received: September 6, 2021
Accepted: December 2, 2021

DOI: 10.22146/ijc.68599

Abstract: *Kaolinite is an essential mineral with numerous applications across many sectors. One of them is in the agricultural industry, in which it is a crucial component in the method of controlled-release fertilizer. This manuscript reports the use of different functionals and basis sets on the structural and electronic properties of kaolinite's surface, intending to find reliable methods among those tested. Four different functionals, B3LYP, CAM-B3LYP, M06-2X, TPSSTPSS, complemented with various basis sets, were used in this study. The results show that TPSSTPSS complement with 6-311G** provides good agreement with previous research and experimental results among different functionals and basis sets used. The quantitative analysis was done to optimize the kaolinite molecule. Selected extrema points were used to place the urea molecule for the interaction of urea-kaolinite studies. The urea's interaction with kaolinite was reported at a different interaction site in the gas phase and different orientations of the urea molecule. Urea molecule was optimized above the Al–O and Si–O surfaces with their energy difference calculated. Our results showed that both surfaces act as promising adsorbents among the different orientations of the urea on both the Al–O and Si–O surfaces. However, Al–O, and Si–O had another preferable interaction site to the urea molecules.*

Keywords: *Density functional theory; kaolinite; urea; electrostatic potential surface; kaolinite-urea interaction*

■ INTRODUCTION

Nowadays, controlled-release fertilizers (CRF) have become a new trend to minimize environmental pollution. CRF can control and delay the nutrients release in synchrony with the sequential needs of the plants. Thus, this type of fertilizer will enhance the efficiency of the uptake of the nutrients. Engineering designs are searching for an inexpensive chemical mineral that can be modified to achieve their target as CRF. Kaolinite is one of the materials that still generate interest in different research fields [1-5]. Kaolinite has been chosen as the nanostructure material to act as CRF due to its ability to reduce nutrient losses, increase nutrient-used efficiency and protect the environment [6-12].

Kaolinite has a layer with a large active surface area. Therefore, it can be exploited to enhance surface interaction with fertilizer elements. Kaolinite with chemical formula $Al_2Si_2O_5(OH)_4$, as shown in Fig. 1, is a 1:1 dioctahedral phyllosilicate compound. A single-layer of kaolinite is a SiO_4 tetrahedral sheet and AlO_6 sheet, connected by oxygen atoms between the sheets. One hydrogen atom is bonded to the oxygen between the sheets (inner hydroxyl). In contrast, the other six hydrogen atoms are associated with the oxygen at the lower side of the AlO_6 sheet. This O–H is usually known as inner surface hydroxyl.

This paper focuses on both surfaces of AlO_6 (Al–O) and SiO_4 (Si–O) as they can function as H-acceptors in forming H-bonds to drive the intercalation of molecules [8].

Brindley and Robinson first reported the crystal structure of kaolinite (with non-H atoms) using powder X-ray diffraction [13]. However, earlier stages of research on kaolinite, show conflicting results on the structure of kaolinite, which then solved with space group C1 on both theoretical and experimental studies [14].

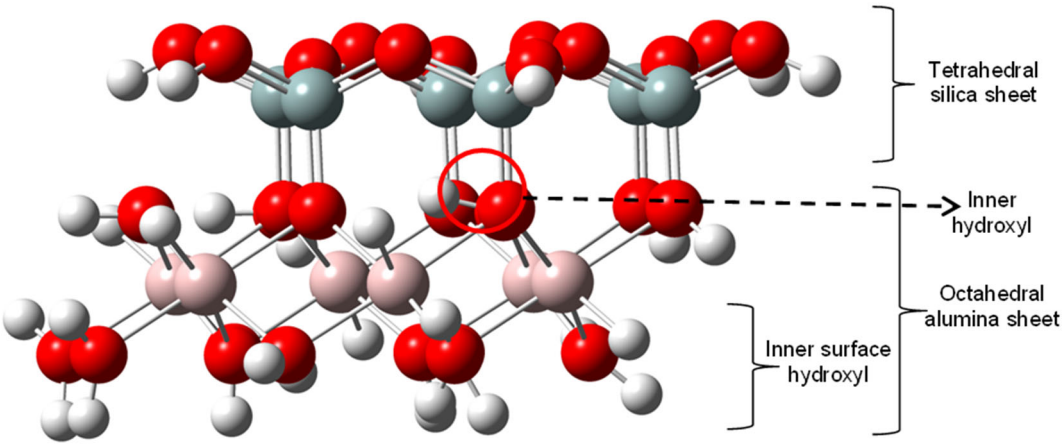

Fig 1. Kaolinite of one ring of the SiO_4 tetrahedral attached with one ring of the AlO_6 octahedral sheets (Red = oxygen, grey = silicon, pink = aluminum, and white = hydrogen)

Silicon, aluminum, and oxygen atoms' positions had resolved from the experimental view, except the determination of the exact positions of hydrogen, which is limited by the technique used. Furthermore, the weak interaction of X-rays with hydrogen atoms makes them unable to provide accurate hydrogen position information. The discrepancy of the experimental results could be due to different sample environments, sources of samples, and refinement methods. However, results from Bish et al. from the diffraction experiment have become a marker for computational studies [15].

Theoretical studies using the ab initio method or density functional theory have been performed on the atomic structure of kaolinite to complement the experimental data [14,16-22]. Here we focus on the hydroxyl bonds of the kaolinite's surface as they are responsible for the adsorption with external molecules. Table 1 shows the different computational methods used with their hydroxyl bond lengths compared to the experimental data from Bish et al. study [15]. B3LYP function was used twice in the previous calculation where the kaolinite material used is in cluster compound [18-19]. It is convinced that B3LYP was more reliable functional than other DFT methods when dealing with OH group vibrational properties, especially when hydrogen bonds are present [19]. Castro and Martin studied different kaolinite sizes where no significant result showed affected from different sizes. Improvement of the basis set was made later. However, only inner hydroxyl bond length has a length different ~0.01 Å

Table 1. Hydroxyl bond length (in Å) from previous theoretical studies of kaolinite

	Experimental Study	Computational Study						
	Bish et al. [20]	Hess and Sauders [21]	Hobbs et al. [23]	Balan et al. [22]	Castro and Martin [23]	Tosoni et al. [24]	Hu and Michaelides [25]	White et al. [16]
Computational method		HF/STO-3G HF/6-21G	CA-PZ/DZP	PBE/PW	RHF/3-21G*, B3LYP/3-21G* At different sizes of kaolinite	B3LYP/6-31G**	PBE/PW	GGA-BLYP/DNP
Inner hydroxyl bond lengths	0.974	0.99	0.994	0.980	0.962–0.993	0.969	0.974	0.974
Inner surface hydroxyl bond lengths *	0.976 0.983 0.979		0.991	0.975	0.963–0.987	0.964 0.965 0.962	0.969 0.970 0.969	0.972 0.970 0.970

*Some paper gives three different bond lengths for inner surface hydroxyl bond length

compared to Bish et al., while others are not much different from previous results. PBE was another function that was repetitively used in previous studies. It routinely predicts hydrogen bond strength better than the results obtained from other quantum chemistry methods with a large basis set. Results also show that PBE has less bond length than Bish et al. bond length than B3LYP functional results.

Besides confirming the kaolinite structure, research on the interaction between kaolinite's surface with guest molecules is also of interest [2,24-29]. Two types of approaches were used previously, either a) periodic model where the kaolinite is infinite, and calculation of interaction is in bulk view [2,24,28], and b) kaolinite is modeled with finite-size clusters [25-27,29-30]. For both approaches, urea is known as one of the guess molecules used to interact with the kaolinite for CRF purposes [11]. Therefore, an experimental-based study was done to find the properties of the urea-kaolinite compound [31-33]. Furthermore, further investigation by the computer simulation was done concerning the possible orientation of urea in the kaolinite-urea intercalation complex. It was pointed out that the dipole moment vectors of urea molecules tend to point towards the silica sheet. Thus, the character of the hydrogen bonds can be described more precisely in simulation [28,34]. However, these studies were done in a bulk mode where kaolinite is infinite, and many urea molecules are intercalated between kaolinite structures.

For this manuscript, the finite size of the kaolinite structure, as shown in Fig. 1, was applied. Previous studies have shown that systematically clustering a structure would lead its energy closer to the experimental values as the structure goes bigger [35]. However, the finite structure still gives out the same interaction potential as infinite structure [34]. To have systems that can react as infinite structures, commonly used in the theoretical study, is by terminating the dangling bond of the structure with hydrogen [2,24,28]. Thus, this article is set to build a kaolinite cluster model and further explore the adsorption properties of urea on the kaolinite surface.

■ COMPUTATIONAL DETAILS

For this study, the kaolinite structure is taken from Bish et al. [15], where the structure of kaolinite is of a triclinic cell and belongs to the C1 space group (sub-class point group of triclinic crystal system). This study used a single ring of Si–O combined with a single ring of Al–O to represent the Si–O sheet and Al–O sheet of kaolinite, respectively. Dangling bonds were terminated by hydrogens, resulting in 72 atoms of kaolinite used in this study. The hydroxyl positions were completely optimized while other atoms were frozen to their original positions. The inner hydroxyl was labeled as $OH_{11\text{-}12}$ between the tetrahedral silica and octahedral alumina sheets. The inner surface hydroxyls are the hydrogen under octahedral alumina sheet was labeled as $OH_{13\text{-}14}$, $OH_{20\text{-}28}$, $OH_{19\text{-}38}$, $OH_{33\text{-}47}$, $OH_{42\text{-}48}$, and $OH_{51\text{-}52}$. Urea molecule was added at three different initial positions of the geometrically relaxed kaolinite cluster to study the interaction between the kaolinite and urea. Only the interaction site and urea were fully optimized, while other atoms were frozen throughout the calculation. Interaction sites are sites that are adjacent to the urea molecule. For example, as urea was placed on top of Si–O, only hydroxyl of Si–O, and urea were optimized. For this investigation, we assessed the capability of different sites to absorb urea molecules. However, only four of the most stable configurations were selected for analysis.

Different functionals of B3LYP, CAM-B3LYP, M06-2X and TPSSTPSS as implemented in Gaussian09 [36] combined with different basis sets (6-31G, 6-31G(d), 6-31G(d,p), 6-311G(d,p), 6-311++G(d,p) and DEF2-TZVP) were used in this study. The inclusion of the functional B3LYP with the 6-31G(d) basis set is due to its extreme popularity in adsorption on clay minerals and proper function for electrostatic interaction [25-27,29]. CAM-B3LYP functional is said to be advancement functional of B3LYP in the long-range calculation [37]. M05-2X was discussed in a previous study able to complement the result of B3LYP [38]. However, the newer and improved M06-2X had a lower bond length error than the M05-2X [39]. Thus, this study included these functions in the calculation of kaolinite. The interaction energy (IE) of optimized structure is calculated as the difference between the total

energy of complex and the whole energies of two separate molecules. The basis set superposition error (BSSE) was corrected by the empirical counterpoise method, and treatment of dispersion is included in this study. [40]. D3BJ gives less average error than non-dispersion corrected calculation and D3 dispersion-corrected DFT scheme [41]. The approach used in the current work can be referred to in our previous work [42].

■ RESULTS AND DISCUSSION

Energy Study

Fig. 2(a) shows the bond length of hydroxyl calculated in the gas phase with different basis set in B3LYP functional. All the hydroxyl bond lengths obtained are shorter than the Bish et al.. The smallest size basis set used in this study, 6-31G, produces the closest

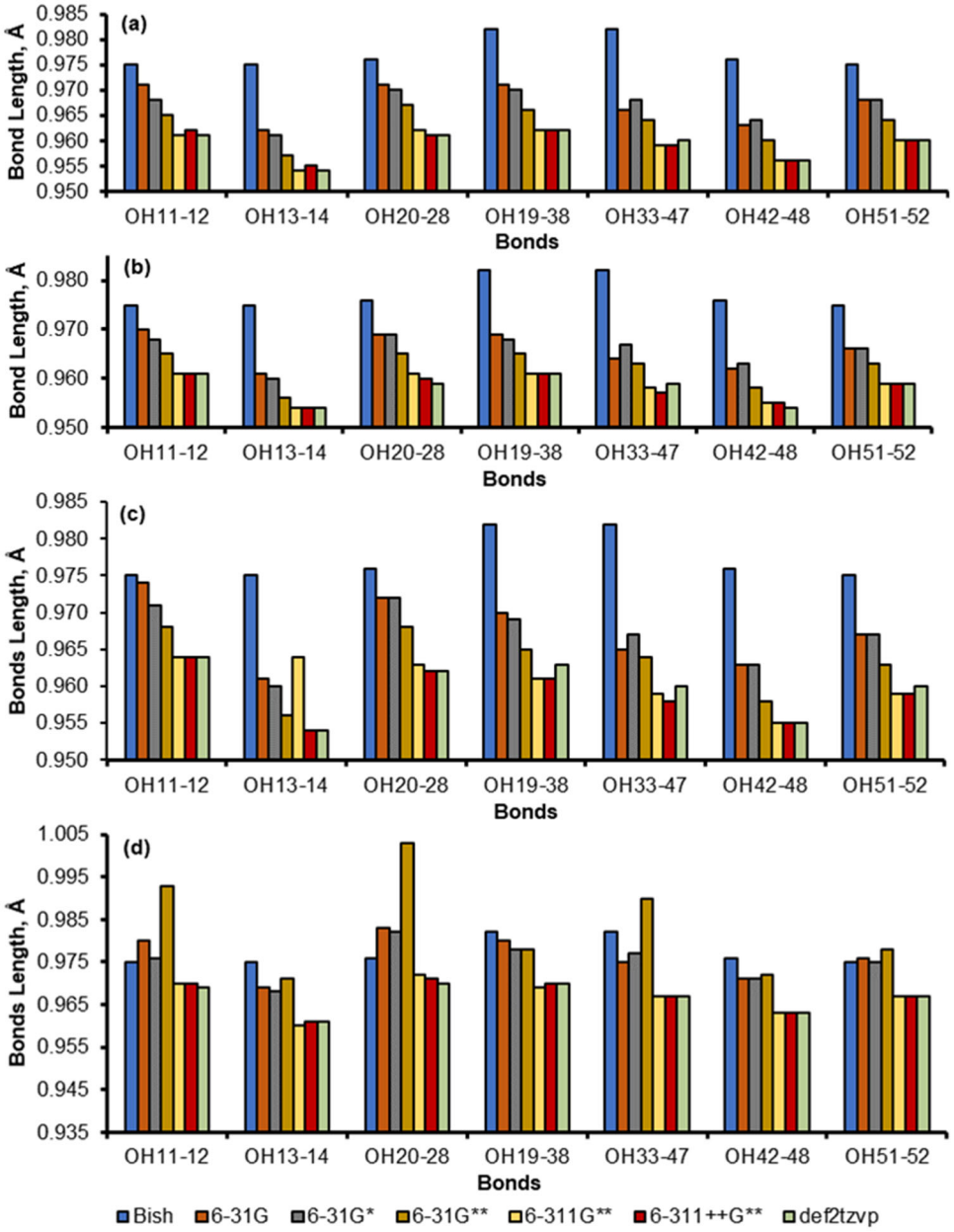

Fig 2. Hydroxyl bond lengths from different functionals and different basis sets. There are six basis sets being complemented with (a) B3LYP, (b) CAM-B3LYP, (c) M06-2X, and (d) TPSSTPSS functionals. The experimental value from Bish et al. is also included for comparison

value of experimental inner hydroxyl bond length (OH_{11-12}, 0.971 Å against 0.974 Å from Bish), compared to other larger basis sets used. Compared to the previous study of Tosoni et al. and Castro and Martin, the inner hydroxyl from B3LYP/6-31G in this study has the closest bond length to the experimental value [18-19]. For the inner surface hydroxyl bond in this study, the bond length is still in the same range as the previous research. Including polarization function (single or double) to this double zeta basis set shorten this bond length by about 0.007 Å at 6-31G* and by 0.010 Å at 6-31G**. The three triple zeta basis sets of 6-311G**, 6-311++G**, and DEF2-TZVP produce similar or equal bond lengths as the bar chart is flat. However, the bond length is 0.015 Å to 0.022 Å shorter than Bish et al.'s reported values. Adding diffuse function (++) to the triple zeta basis set does not provide any significant changes to the hydroxyl bond lengths if there are any at all. The results in Fig. 2(a) can be interpreted as the triple zeta basis set "stabilizes" the hydroxyl bond lengths, starting with 6-311G**.

Calculation using a different basis set with CAM-B3LYP, M06-2X, and TPSSTPSS functionals are shown in Fig. 2(b), 2(c), and 2(d). As is the case of B3LYP, all calculation of CAM-B3LYP and M06-2X functionals always has a bond length shorter than the experimental results. The same observations for B3LYP are also applicable here: for higher basis set 6-311G**, 6-311++G** and DEF2TZVP, hydroxyl bond lengths are a similar length and can be considered as consistent, and the diffuse and polarization functions do not give significant effect to the hydroxyl bond length.

Compared to the other functionals used, a few hydroxyl bond lengths under TPSSTPSS are more significant than the reported values. For example, double zeta basis set 6-31G** always resulted in the hydroxyl bond length longer than the experimental bond length, while the over- and under-estimation using 6-31G and 6-31G* are insignificant. Thus, the double zeta basis set provides fluctuated bond lengths and is unsuitable for describing the hydroxyl bond's length for the functional TPSSTPSS. However, the overall hydroxyl bond lengths of TPSSTPSS triple zeta basis sets are closer to the reported experimental values. The range difference is 0.006 to 0.015 Å, lower than the other functionals considered.

Fig. 3 shows the effect of the different functionals on the hydroxyl bond lengths, at basis set 6-311G**, since triple zeta basis set of 6-311G**, 6-311++G**, and DEF2TZVP do not show significant changes in the bond lengths (as seen in Fig. 2–3). Of the four functionals considered in this study, TPSSTPSS has the most hydroxyl bond length, similar to the experimental. For inner surface hydroxyl, this results still in the range with previous study bond length (refer to Table 1) as the hydroxyl bond length range from 0.961 –0.971 Å. From this result, it shows that study on the kaolinite hydroxyl bond is reliable by using one ring with TPSSTPPS/6-311G** method.

A Quantitative Study of Kaolinite Electrostatic Surface Potential

The electrostatic potential (ESP) map is an essential

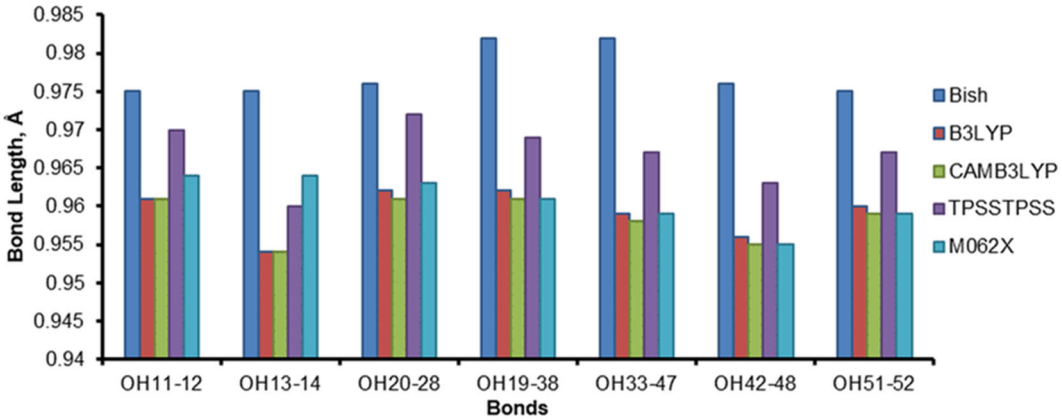

Fig 3. Graph of various functional (basis set was fixed to 6-311G**)

tool for determining the physicochemical properties and explaining the interaction between molecules. However, in this report, an improvement of the potential map discussion for interaction between kaolinite and guess molecules was made. For the adsorption process of organic molecules, the ESP on the surface regions can provide information on the preferable site of the adsorption process. In Gaussview, ESP is represented using colors ranging from blue to red, in which blue indicates a positive surface, red is negative, and green is a neutral charge surface. The color represents the range of charges on the surface of kaolinite. This study also provides the maximum and minimum ESP values from the saddle point of energy range for maximum and minimum surfaces, as given in Table 2. The positive value in Table 2 shows that the site has less charge than the other place, and the negative value has more charges than the different areas of the map.

Fig. 4 shows the ESP surface of single ring kaolinite at Al–O top, Si–O top, and side views. It can be seen in Fig. 4 that the Si–O surface has a more robust red color surface compared to the Al–O surface, which indicates that the Si–O is an electron-deficient surface. It is due to the oxygen atoms on the Si–O surface. For the Al–O surface, the color varied from blue to yellow-reddish. Color changes are due to the structure of the Al–O surface having a variety of hydroxyl orientations. Some of the hydroxyls point out the kaolinite, shown as the blue surface, while others point to the middle of the kaolinite ring. For hydroxyl pointing to the center, the energy contribution was included with sites atom (Al–O) and shown as yellow-reddish colored, which is less negative. Orientation of the hydroxyl at the Al–O was similar to previous experimental study results [43-44]. The middle ring hydroxyl of inner surface hydroxyl had tilted toward an empty octahedral site with one of it almost horizontal.

From Table 2, the maximum point appears more on the Al–O surface than the Si–O surface. The maximum points for Al–O surface are positive, ranging from 1.38 to 1.43 eV, while Si–O has a negative value of –0.60 eV for its maximum point. Minimum ESP value shows Al–O surface has energy range from –1.44 to 0.42 eV while Si-O surface has lower energy range from –2.04 to –1.86 eV. Energy differences on different surfaces indicate that the Al–O surface is an electron-abundant surface while Si–O is an electron-deficient kaolinite surface.

Table 2. Quantitative ESP energy of the kaolinite ESP surface

Site	Energy (eV)			
	Position	Maximum	Position	Minimum
Al–O	1	1.4094	1	0.4152
	2	1.3758	2	–1.2651
	3	1.4287	3	–1.4390
Si–O	1	–0.5923	1	–1.8637
			2	–2.0377
			3	–1.8642
			4	–1.9476

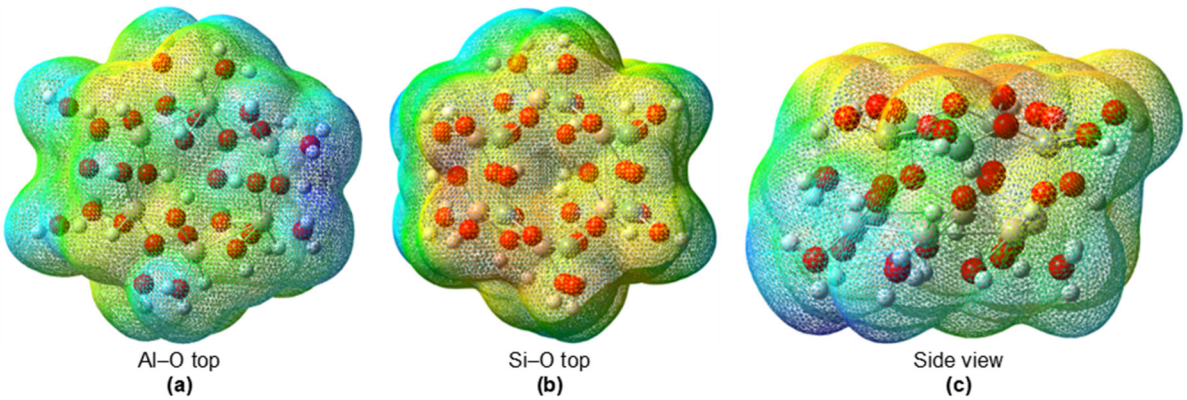

Fig 4. The ESP surface of the kaolinite

The location of the urea to study the interaction of kaolinite with urea is predicted using these extrema points in Table 2 and pointed as shown in Fig. 5. The extrema point always appears in the middle of the ring for both the Si–O surface and the Al–O surface. Maximum points are shown at the Al–O surface hydroxyl, specifically on top of hydrogens. As shown in Fig. 5, four hydroxyls exist in the middle of the kaolinite ring. However, only three hydroxyls had a maximum point which is OH_{51-52}, OH_{13-14}, and OH_{19-36}. As mentioned before, OH_{20-28} is the hydroxyl that points to the middle of the kaolinite ring. Thus, at that site, the ESP energy on the surface is a combination of all-atoms at the hydroxyl side. The difference in orientation of hydroxyl affects their function as H-donor and H-acceptor. Minimum points are shown in the ring of Si–O, which was previously shown to act as a proton-acceptor when interacting with the guest molecule [29]. From this observation, it is predicted that the urea will interact at these extrema points. Thus, urea is placed on top of these extrema points and optimized. The proportion and energetic results are shown in Table 2 and Fig. 6.

Interaction of Kaolinite with Urea

Our qualitative and quantitative calculations of the ESP have confirmed preferential adsorption sites for urea on kaolinite surfaces. As mentioned in ESP results, the preferable interaction site is at the middle of the Al–O and Si–O ring surface. Thus, urea was placed on the top of the surfaces and optimized. Optimized structures of urea and kaolinite are shown in Fig. 6, and energetic results are in Table 3. This study compares urea with individual Al–O and Si–O sheets and urea with kaolinite at different Al–O and Si–O surfaces. In Table 2, individual sheets of Si–O and Al–O interacting with urea are labeled as Si–O + urea and Al–O + urea. While kaolinite sheets interact with urea at the different surfaces are labeled as kaolinite + urea, with a bracket including the interaction surface (Al–O or Si–O).

Generally, Table 2 shows that all interaction involved has negative interaction energy, indicating that both surfaces can adsorb urea as suggested previously [2]. For the Al–O surface, interaction energy ranges from –0.9904 to –1.5825 eV, while –0.4252 to –0.6040 eV for the Si–O surface. Different energy shows that the Al–O surface has higher interaction energy than the Si–O surface, depicting that the urea prefers to attach at the Al–O sheet surface than the Si–O sheet surface. The previous experimental studies reported that urea prefers interaction at the Si–O sheets and suggest that it is due to the dual NH_2 of urea from the Raman and vibration view [31-32]. However, thermal study on this complex shows at the cooler temperature, the urea and hydroxyl surface of Al–O are brought closer together so that hydrogen bonding between the hydroxyls of the gibbsite-like layer of the Al–O sheet and the C=O group

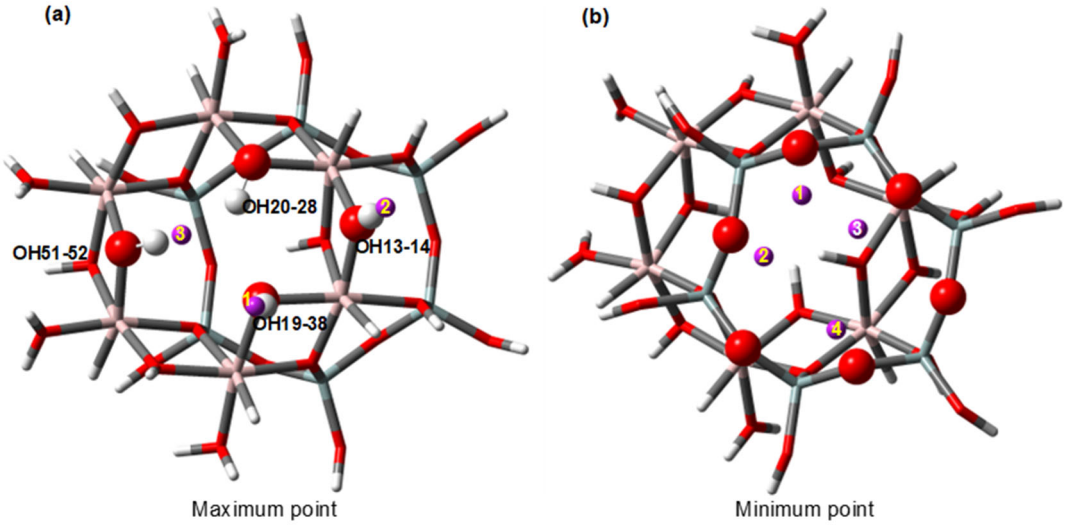

Fig 5. The minimum and maximum points on the Al–O, and Si–O surfaces. (Purple is the extrema point)

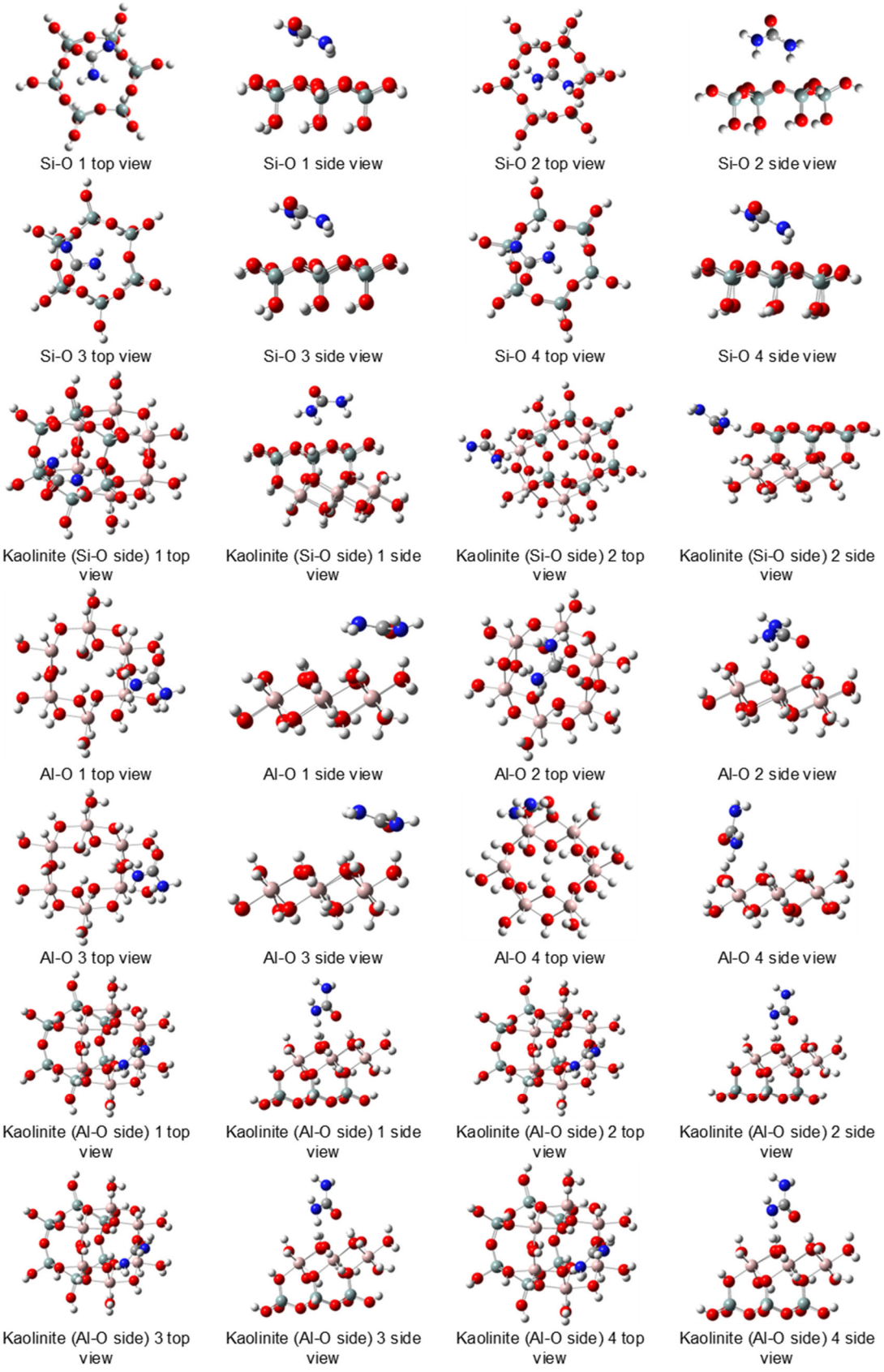

Fig 6. The optimized structures of kaolinite-urea clusters

Table 3. Interaction energy (IE) and the hydrogen bond

Structure	Position	eV	Bond Type	Bond Length (Å)
Si–O + urea	1	-0.4529	N–H···O	2.6503
			N–H···O	2.6351
			N–H···O	2.3759
	2	-0.4252	N–H···O	2.2928
			N–H···O	2.4523
	3	-0.4733	N–H···O	2.6474
			N–H···O	2.6891
			N–H···O	2.3613
	4	-0.5012	N–H···O	2.4520
			N–H···O	2.4132
			N–H···O	2.3130
Al–O + urea	1	-1.3835	O···H	1.7870
			N···H	1.7764
	2	-1.5825	O···H	1.7649
			N···H	2.2388
			N–H···O	1.9850
	3	-1.2458	N···H	1.8206
			O···H	1.7319
			N···H	2.8443
	4	-0.9904	N···H	2.3649
			O···H	1.8226
Kaolinite (Si–O side) + urea	1	-0.5052	N–H···O	2.6066
			N–H···O	2.7972
			N–H···O	2.4232
	2	-0.6040	O···H	2.1182
			N–H···O	2.5268
			N–H···O	2.1877
Kaolinite (Al–O side) + urea	1	-0.4781	O···H	1.9694
			N–H···O	1.8706
			O···H	2.0968
	2	-1.0172	O···H	1.9690
			O···H	2.0971
			N-H···O	1.8704
	3	-1.0013	O···H	1.9635
			O···H	2.1318
			N–H···O	1.8863
	4	-1.0170	O···H	1.9692
			O···H	2.0967
			N–H···O	1.8704

of urea can occur [32]. Simulation study on the different amide molecules attached at the kaolinite also shows that these molecules had higher interaction energy at the Al–O sheet than at the Si–O sheet [25,27,38]. As shown in Table 3, the bond length for urea interacting with the hydroxyl of Al–O is shorter than the bonding at the Si–O sheet. Primary interaction at the Al–O sheet is from the N–H of urea with oxygen from hydroxyl of gibbsite layer with bond length 1.87–1.99 Å. Secondary interaction is between oxygen and nitrogen atoms of the urea with the hydroxyl of the Si–O sheet.

The interaction sites are as conveyed by the ESP surface, where the red ESP map surface had attracted the dual NH_2 of the urea molecule to the basal oxygen on the siloxane surface (N–H···O). The hydrogen bonding of N–H···O bond length is in the range of 2.3–2.8 Å on the Si–O surface and did complement the previous study on the interaction between urea and kaolinite [2]. The ESP surface map had varying colors from blue to green on the Al–O sheet, which was predicted to act as H-donor and H-acceptor. The results from Table 3 and Fig. 6 had shown on the Al–O sheet, and both interactions are involved. The hydroxyl that points outward of the kaolinite sheet (appear blue in Fig. 4) acts as the H-acceptor by interacting with the oxygen and nitrogen from the urea molecules. At the same time, the other hydroxyl interacts with the NH_2 of the urea molecule as H-donor when they point to the middle of the kaolinite ring [2].

The previous studies had already discussed that the orientation of the guess molecule, when placed at the different sites of kaolinite, would appear differently. 2,4-dinitrotoluene on kaolinite surface change from dihedral angle 60° at Al–O sheet to 10° at the Si–O sheet, resulting from the hydrogen bond between the guest molecule and kaolinite sheets [29]. Fig. 6 shows that urea molecule orientation after optimization on top of the Si–O and Al–O appeared parallel or perpendicular to the kaolinite sheet. A simulation study using molecular dynamic simulation had reported in infinite structure, few urea molecules are nearly parallel to the basal surface of kaolinite, with the urea molecules situated closer to the silica tetrahedron sheet. Meanwhile, some urea molecules are almost perpendicular to the basal surface of kaolinite [45]. Simulation study of bulk amount of urea on top of infinite Si–O sheet shows that final orientation of urea is always almost parallel to the sheets with the angle between 0°–20° [28]. Urea on top of the Si–O sheet, as shown in Fig. 6, also had a similar orientation as reported in previous experimental and simulation studies with dual hydrogen bonding [32]. The orientation at the Al–O had never been reported previously. This study simulated the closeness of both molecules oriented the urea perpendicular to the top of the Al–O surface. In this position, one N–H bond interacts with the hydroxyl of Al–O and the other N–H bond of urea free on the other side, as in Fig. 6.

Interaction between urea and kaolinite in simulation is scarce compared to other molecules. For other molecules studied in the finite structure of kaolinite, it always includes the single sheets of Al–O or Si–O to find the interaction between kaolinite and guest molecule [25-27,29]. Thus, this study compared the simulation result with previous research on urea and kaolinite. Results show that for the Si–O surface of kaolinite, urea is the least favorable to finalize on top of the Si–O surface when the single ring of kaolinite is introduced. However, the urea is consistently optimized in the middle of the siloxane ring when an individual Si–O sheet is used. All urea is also in the parallel orientation to the Si-O surface. The interaction energy is higher when a particular Si–O sheet is used due to the minor atom interacting with the urea. Urea had an inconsistent position when only the Al–O sheet was used. The urea tends to have a final position at the side of the kaolinite with both parallel and perpendicular orientation to the Al–O sheet. However, for urea introduced to the kaolinite (Al–O), it can consistently be optimized on the middle of the Al–O ring with perpendicular orientations.

■ CONCLUSION

This work aims to build a kaolinite cluster model and to explore the adsorption on the kaolinite surfaces. It is performed with updated functional and basis set for future references. For the geometry, among different

functionals and basis sets previously used, TPSSTPSS combined with 6-311++G** showed the best result compared to the experimental result. As other studies always used the hydroxyl bond length as a benchmark of comparison, our result also has the hydroxyl bond length values in good agreement with the DFT computations of the previous finding, using bulk and cluster calculations. For the preferable sites of interactions with the guest molecules, Si–O was electron-deficient while the Al–O was an electron-abundant surface. Both Si–O and Al–O surfaces are suitable adsorbent surfaces for guest molecule interaction with kaolinite, compared to the energy of both surfaces interacting with urea. Interaction using urea as guest molecules shows that Si–O is an electron-deficient surface. Thus oxygen of urea is preferred to be attached to it, and Al–O is the dual adsorbent surface where it can interact with oxygen and hydrogen of urea.

■ ACKNOWLEDGMENTS

The Minister of Higher Education Malaysia financially supports this research through the Fundamental Research Grant Scheme (FRGS, project code 600-IRMI/FRGS 5/3 (115/2019)).

■ AUTHOR CONTRIBUTIONS

The authors contributed equally to this work.

■ REFERENCES

[1] Zhang, S., Liu, Q., Cheng, H., and Zeng, F., 2015, Combined experimental and theoretical investigation of interactions between kaolinite inner surface and intercalated dimethyl sulfoxide, *Appl. Surf. Sci.*, 331, 234–240.

[2] Zhang, S., Liu, Q., Gao, F., Li, X., Liu, C., Li, H., Boyd, S.A., Johnston, C.T., and Teppen, B.J., 2017, Mechanism associated with kaolinite intercalation with urea: Combination of infrared spectroscopy and molecular dynamics simulation studies, *J. Phys. Chem. C,* 121 (1), 402–409.

[3] Makó, É., Kovács, A., Katona, R., and Kristóf, T., 2016, Characterization of kaolinite-cetyltrimethylammonium chloride intercalation complex synthesized through eco-friend kaolinite-urea pre-intercalation complex, *Colloids Surf., A*, 508, 265–273.

[4] Táborosi, A., Kurdi, R., and Szilágyi, R.K., 2014, Adsorption and intercalation of small molecules on kaolinite from molecular modelling studies, *Hung. J. Ind. Chem.*, 42 (1), 19–23.

[5] Zhang, S., Gao, N., and Liu, K., 2021, Insights on the intercalation mechanism of the coal-bearing kaolinite intercalation based on experimental investigation and molecular dynamics simulations, *Chem. Pap.*, 75 (12), 6335–6344.

[6] Azeem, B., KuShaari, K., Man, Z.B., Basit, A., and Thanh, T.H., 2014, Review on materials & methods to produce controlled release coated urea fertilizer, *J. Controlled Release*, 181, 11–21.

[7] Roshanravan, B., Mahmoud-Soltani, S., Mahdavi, F., Abdul Rashid, S., and Yusop, M.K., 2014, Preparation of encapsulated urea-kaolinite controlled release fertiliser and their effect on rice productivity, *Chem. Speciation Bioavailability*, 26 (4), 249–256.

[8] Sempeho, S.I., Kim, H.T., Mubofu, E., Pogrebnoi, A., Shao, G., and Hilonga, A., 2015, Dynamics of kaolinite-urea nanocomposites via coupled DMSO-hydroxyaluminum oligomeric intermediates, *Indian J. Eng. Mater. Sci.*, 2015, 920835.

[9] Vejan, P., Khadiran, T., Abdullah, R., and Ahmad, N., 2021, Controlled release fertilizer: A review on developments, applications and potential in agriculture, *J. Controlled Release*, 339, 321–334.

[10] Fariba, M., Suraya, A.R., and Yusop, M.K., 2014, Intercalation of urea into kaolinite for preparation of controlled release fertilizer, *Chem. Ind. Chem. Eng. Q.*, 20 (2), 207–213.

[11] Roshanravan, B., Mahmoud-Soltani, S., Rashid, S.A., Mahdavi, F., and Yusop, M.K., 2015, Enhancement of nitrogen release properties of urea–kaolinite fertilizer with chitosan binder, *Chem. Speciat. Bioavailab.*, 27 (1), 44–51.

[12] de Macedo Neto, J.C., do Nascimento, N.R., Bello, R.H., de Verçosa, L.A., Neto, J.E., da Costa, J.C.M., and Diaz, F.R.V., 2022, Kaolinite review:

Intercalation and production of polymer nanocomposites, *Eng. Sci.*, 17, 28–44.

[13] Brindley, G.W., and Robinson, K., 1946, The structure of kaolinite, *Mineral. Mag. J. Mineral. Soc.*, 27 (194), 242–253.

[14] White, C.E., Provis, J.L., Riley, D.P., Kearley, G.J., van Deventer, J.S.J., 2009, What is the structure of kaolinite? reconciling theory and experiment, *J. Phys. Chem. B,* 113(19), 6756-6765.

[15] Bish, D.L., 1993, Rietveld refinement of the kaolinite structure at 1.5 K, *Clays Clay Miner.*, 41 (6), 738–744.

[16] Hess, A.C., and Saunders, V.R., 1992, Periodic ab initio Hartree-Fock calculations of the low-symmetry mineral kaolinite, *J. Phys. Chem.*, 96 (11), 4367–4374.

[17] Balan, E., Saitta, A.M., Mauri, F., and Calas, G., 2001, First-principles modeling of the infrared spectrum of kaolinite, *Am. Mineral.*, 86 (11-12), 1321–1330.

[18] Castro, E.A.S., and Martins, J.B.L., 2005, Theoretical study of kaolinite, *Int. J. Quantum Chem.*, 103 (5), 550–556.

[19] Tosoni, S., Doll, K., and Ugliengo, P., 2006, Hydrogen bond in layered materials: Structural and vibrational properties of kaolinite by a periodic B3LYP approach, *Chem. Mater.*, 18 (8), 2135–2143.

[20] Hu, X.L., and Michaelides, A., 2008, Water on the hydroxylated (001) surface of kaolinite: From monomer adsorption to a flat 2D wetting layer, *Surf Sci.*, 602 (4), 960–974.

[21] Karmous, M.S., 2011, Theoretical study of kaolinite structure; Energy minimization and crystal properties, *World J. Nano Sci. Eng.*, 1 (2), 62–66.

[22] Heimann, J.E., Grimes, R.T., Rosenzweig, Z., and Bennett, J.W., 2021, A density functional theory (DFT) investigation of how small molecules and atmospheric pollutants relevant to art conservation adsorb on kaolinite, *Appl. Clay Sci.*, 206, 106075.

[23] Hobbs, J.D., Cygan, R.T., Nagy, K.L., Schultz, P.A., and Sears, M.P., 1997, All-atom ab initio energy minimization of the kaolinite crystal structure, *Am. Mineral.,* 82 (7-8), 657–662.

[24] Zhang, Z., Liu, J., Yang, Y., Shen, F., and Zhang, Z., 2018, Theoretical investigation of sodium capture mechanism on kaolinite surfaces, *Fuel,* 234, 318–325.

[25] Song, K.H., Zhong, M.J., Wang, L., Li, Y., and Qian, P., 2014, Theoretical study of interaction of amide molecules with kaolinite, *Comput. Theor. Chem.*, 1050, 58–67.

[26] Zhang, C., Qi, Y.H., Qian, P., Zhong, M.J., Wang, L., and Yin, H.Z., 2014, Quantum chemical study of the adsorption of water molecules on kaolinite surfaces, *Comput. Theor. Chem.*, 1046, 10–19.

[27] Song, K.H., Wang, X., Qian, P., Zhang, C., and Zhang, Q., 2013, Theoretical study of interaction of formamide with kaolinite, *Comput. Theor. Chem.,* 1020, 72–80.

[28] Rutkai, G., Makó, É., and Kristóf, T., 2009, Simulation and experimental study of intercalation of urea in kaolinite, *J. Colloid Interface Sci.*, 334 (1), 65–69.

[29] Wang, X., Qian, P., Song, K., Zhang, C., and Dong, J., 2013, The DFT study of adsorption of 2,4-dinitrotoluene on kaolinite surfaces, *Comput. Theor. Chem.*, 1025, 16–23.

[30] Volkova, E., Narayanan Nair, A.K., Engelbrecht, J., Schwingenschlögl, U., Sun, S., and Stenchikov, G., 2021, Molecular dynamics modeling of kaolinite particle associations, *J. Phys. Chem. C*, 125 (43), 24126–24136.

[31] Frost, R.L., Tran, T.H., and Kristof, J., 2018, The structure of an intercalated ordered kaolinite - A Raman microscopy study, *Clay Miner.*, 32 (4), 587–596.

[32] Frost, R.L., Kristof, J., Rintoul, L., and Kloprogge, J.T., 2000, Raman spectroscopy of urea and urea-intercalated kaolinites at 77 K, *Spectrochim. Acta, Part A*, 56 (9), 1681–1691.

[33] Cheng, H., Liu, Q., Yang, J., Ma, S., and Frost, R.L., 2012, The thermal behavior of kaolinite intercalation complexes-A review, *Thermochim. Acta*, 545, 1–13.

[34] Mohd Nabil, N.N.A., Mohd Zabidi, A.R., Abdullah, N.A.F., and Ang, L.S., 2017, Stability and electronic properties of urea in different arrangements: A DFT-based study, *Jurnal Intelek*, 12 (2), 44–54.

[35] Mohd Nabil, N.N.A., and Ang, L.S., 2017, Theoretical investigation of the lattice energy of

urea: Insight from DFT using systematic cluster method, *Malays. J. Fundam. Appl. Sci.*, 13 (4), 632–636.

[36] Frisch, M.J., Trucks, G.W., Schlegel, H.B., Scuseria, G.E., Robb, M.A., Cheeseman, J.R., Scalmani, G., Barone, V., Mennucci, B., Petersson, G.A., Nakatsuji, H., Caricato, M., Li, X., Hratchian, H.P., Izmaylov, A.F., Bloino, J., Zheng, G., Sonnenberg, J.L., Hada, M., Ehara, M., Toyota, K., Fukuda, R., Hasegawa, J., Ishida, M., Nakajima, T., Honda, Y., Kitao, O., Nakai, H., Vreven, T., Montgomery Jr., J.A., Peralta, J.E., Ogliaro, F., Bearpark, M., Heyd, J.J., Brothers, E., Kudin, K.N., Staroverov, V.N., Kobayashi, R., Normand, J., Raghavachari, K., Rendell, A., Burant, J.C., Iyengar, S.S., Tomasi, J., Cossi, M., Rega, N., Millam, J.M., Klene, M., Knox, J.E., Cross, J.B., Bakken, V., Adamo, C., Jaramillo, J., Gomperts, R., Stratmann, R.E., Yazyev, O., Austin, A.J., Cammi, R., Pomelli, C., Ochterski, J.W., Martin, R.L., Morokuma, K., Zakrzewski, V.G., Voth, G.A., Salvador, P., Dannenberg, J.J., Dapprich, S., Daniels, A.D., Farkas, Ö., Foresman, J.B., Ortiz, J.V., Cioslowski, J., and Fox, D.J., 2013, *Gaussian-09 Revision D.01*, Gaussian, Inc., Wallingford, CT.

[37] Yanai, T., Tew, D.P., and Handy, N.C., 2004, A new hybrid exchange–correlation functional using the Coulomb-attenuating method (CAM-B3LYP), *Chem. Phys. Lett.*, 393 (1-3), 51–57.

[38] Michalkova, A., Robinson, T.L., and Leszczynski, J., 2011, Adsorption of thymine and uracil on 1:1 clay mineral surfaces: Comprehensive ab initio study on influence of sodium cation and water, *Phys. Chem. Chem. Phys.*, 13 (17), 7862–7881.

[39] Zhao, Y., and Truhlar, D.G., 2008, The M06 suite of density functionals for main group thermochemistry, thermochemical kinetics, noncovalent interactions, excited states, and transition elements: two new functionals and systematic testing of four M06-class functionals and 12 other functionals, *Theor. Chem. Acc.*, 120 (1), 215–241.

[40] Kruse, H., and Grimme, S., 2012, A geometrical correction for the inter- and intra-molecular basis set superposition error in Hartree-Fock and density functional theory calculations for large systems, *J. Chem. Phys.,* 136 (15), 154101.

[41] Christensen, A.S., Kubař, T., Cui, Q., and Elstner, M., 2016, Semiempirical quantum mechanical methods for noncovalent interactions for chemical and biochemical applications, *Chem. Rev.*, 116 (9), 5301–5337.

[42] Mohd Nabil, N.N.A., and Ang, L.S., 2019, Conformational and topology analysis of diphenylthiourea and diarylhalidethiourea compounds using DFT, *Indones. J. Chem.*, 20 (2), 264–275.

[43] Benco, L., Tunega, D., Hafner, J., and Lischka, H., 2001, Orientation of OH groups in kaolinite and dickite: Ab initio molecular dynamics study, *Am. Mineral.*, 86 (9), 1057–1065.

[44] Giese, R.F., and Datta, P., 1973, Hydroxyl orientation in kaolinite, dictite, and nacrite, *Am. Mineral.*, 58 (5-6), 471–479.

[45] Liu, Q., Zhang, S., Cheng, H., Wang, D., Li, X., Hou, X., and Frost, R.L., 2014, Thermal behavior of kaolinite–urea intercalation complex and molecular dynamics simulation for urea molecule orientation, *J. Therm. Anal. Calorim.*, 117 (1), 189–196.